

Introduction: In sinter process, the fine iron ores are prepared for the blast furnace process by agglomeration at high temperatures. This process allows recycling of waste products from other sections of the steel making process. The efficiency of the process can be improved by permeability bars, which locally increase the porosity of the bed. A transient 2D sinter process model was developed to investigate the influence of various permeability bar configurations on the process.

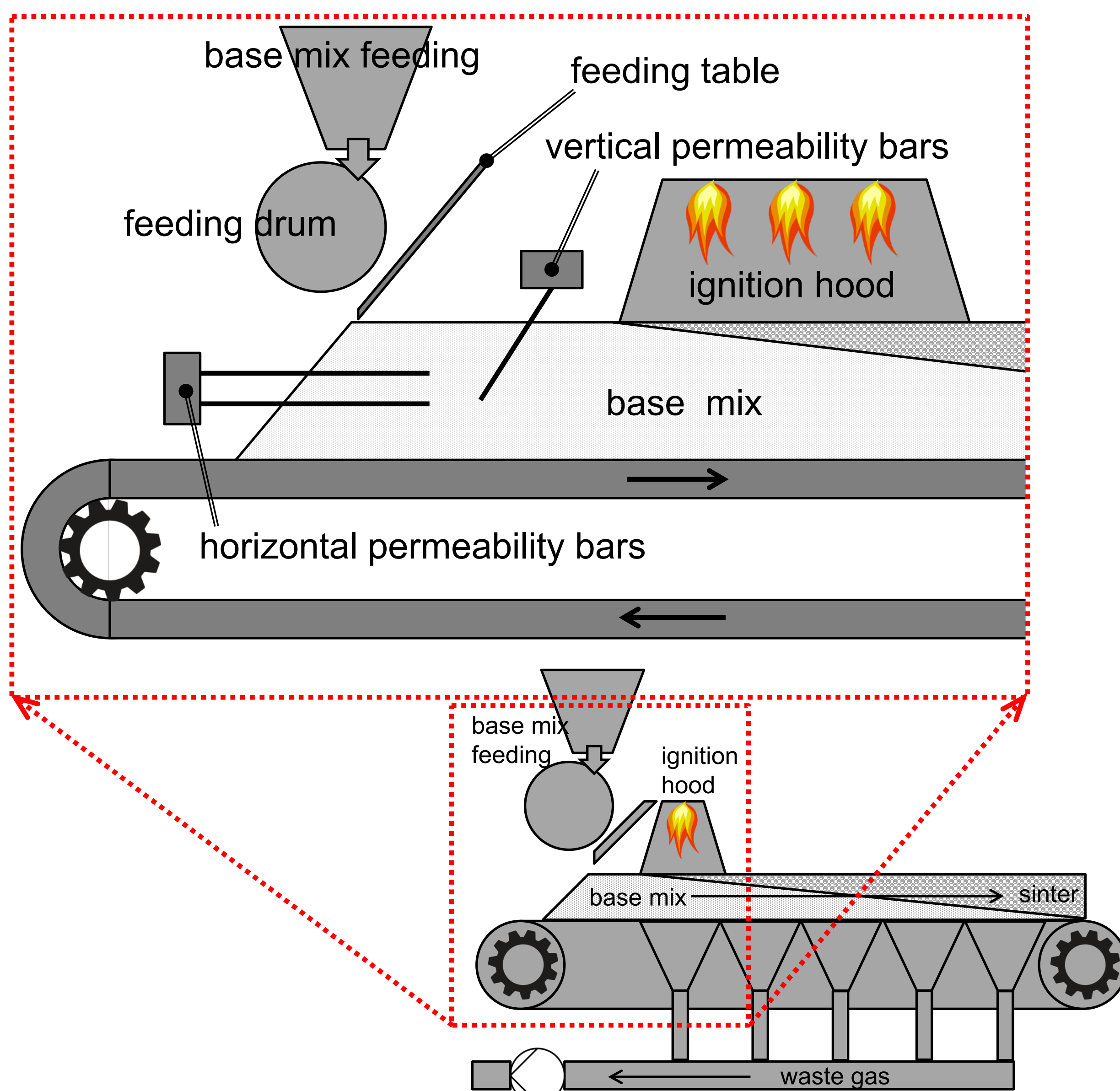


Figure 1. Typical sinter plant base mix feeding system and placement of the horizontal and vertical permeability bars

Computational Methods: The sinter process simulation model presented here solves the reacting flow through porous bed problem. It is essential for this study to model the influence of local permeability changes. In summary, the model includes all of the relevant sub-processes within the sintering process as listed below:

1. heat transfer in gas and solids
2. heat exchange between gas and solids,
3. melting and solidification enthalpies.
4. gas flow through the porous bed,
5. **porosity sub-model,**
6. mass exchange between gas and solids,
7. transport of concentrated species in gas,
8. drying and condensation,
9. coke burn-out, calcination, and sulfation

The porosity sub-model constitutes the crucial part as it defines local permeability and porosity in the base mix.

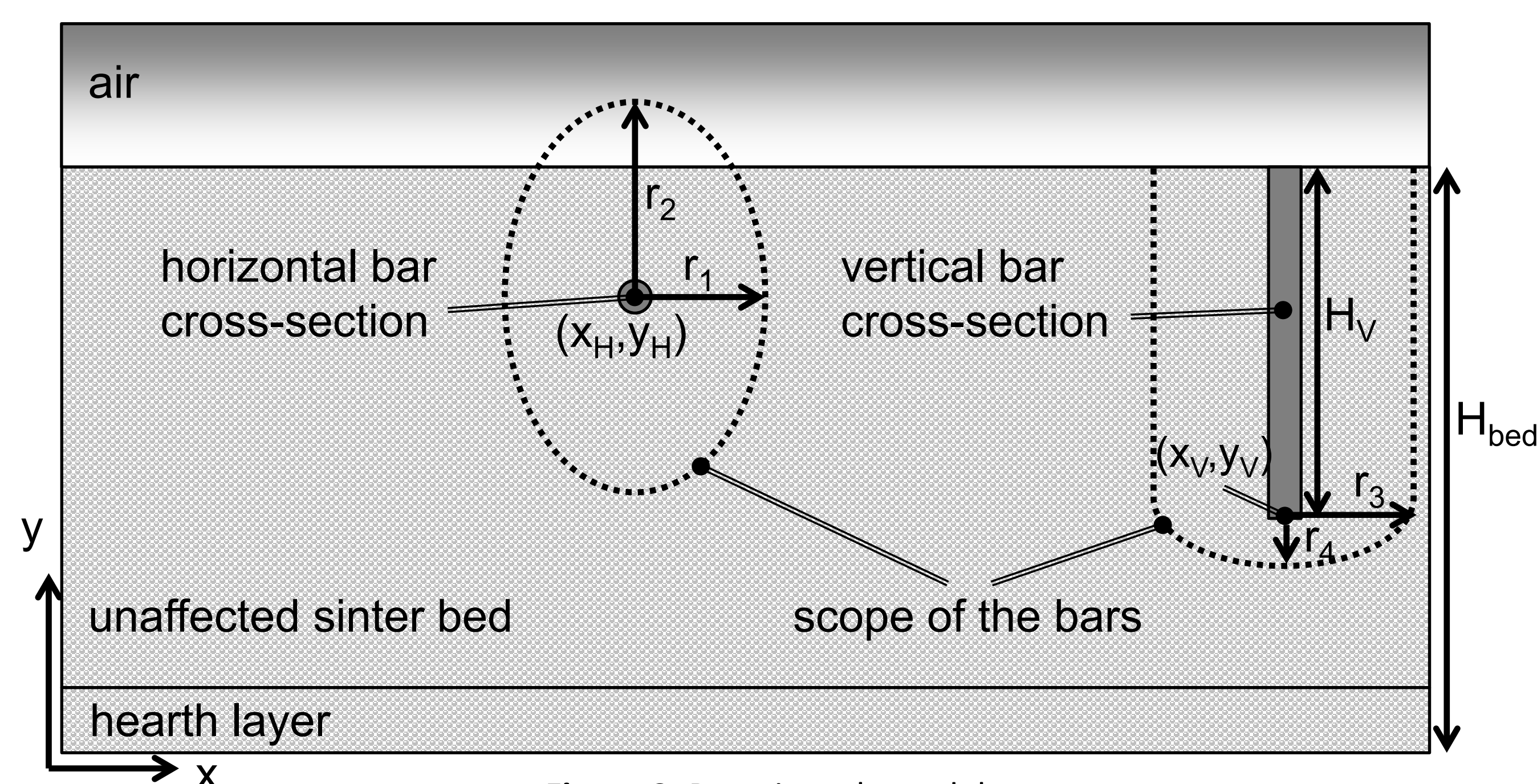


Figure 2. Porosity sub-model

The local porosity distribution is computed by:

$$\epsilon_s(x, y) = \epsilon_{s0} + \Delta\epsilon \cdot (\text{step}(\hat{r}_H^2) + \text{step}(\hat{r}_V^2)) \quad \text{where}$$

$$\hat{r}_H^2 = \begin{cases} \frac{(x-x_H)^2}{r_1^2} + \frac{(y-y_H)^2}{r_2^2} & \text{if } y > y_H \\ \frac{(x-x_V)^2}{r_3^2} + \frac{(y-y_V)^2}{r_4^2} & \text{if } y < y_V \\ \frac{(x-x_V)^2}{r_3^2} & \text{otherwise} \end{cases}$$

Results: The main results which are of interest for the plant operation are the specific energy flow in the sintering process, bed temperature, exhaust gas temperature, coke consumption as well as calcination and sulfation, drying/condensation, and sinter quality.

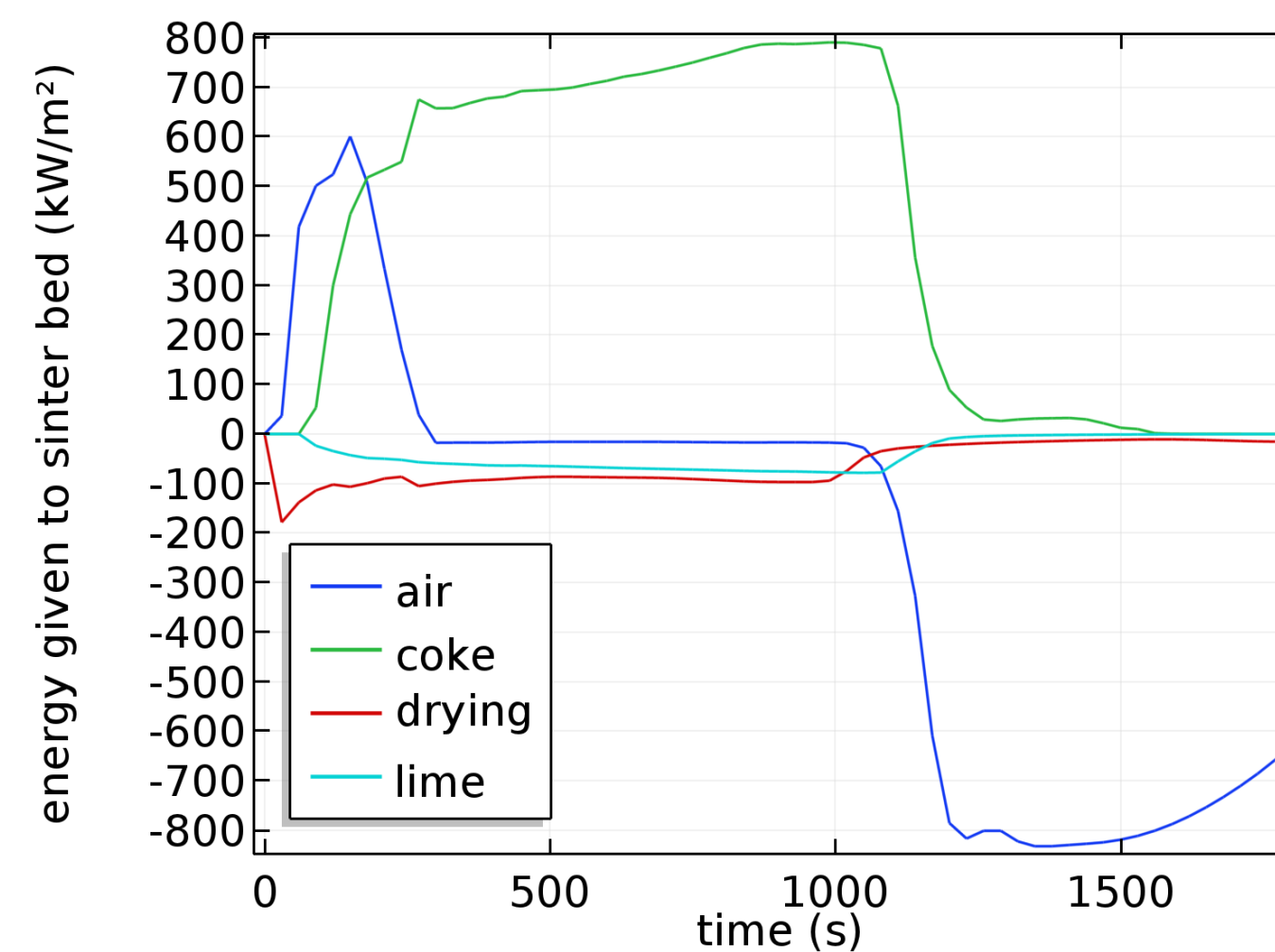


Figure 3. Specific energies given to sinter bed

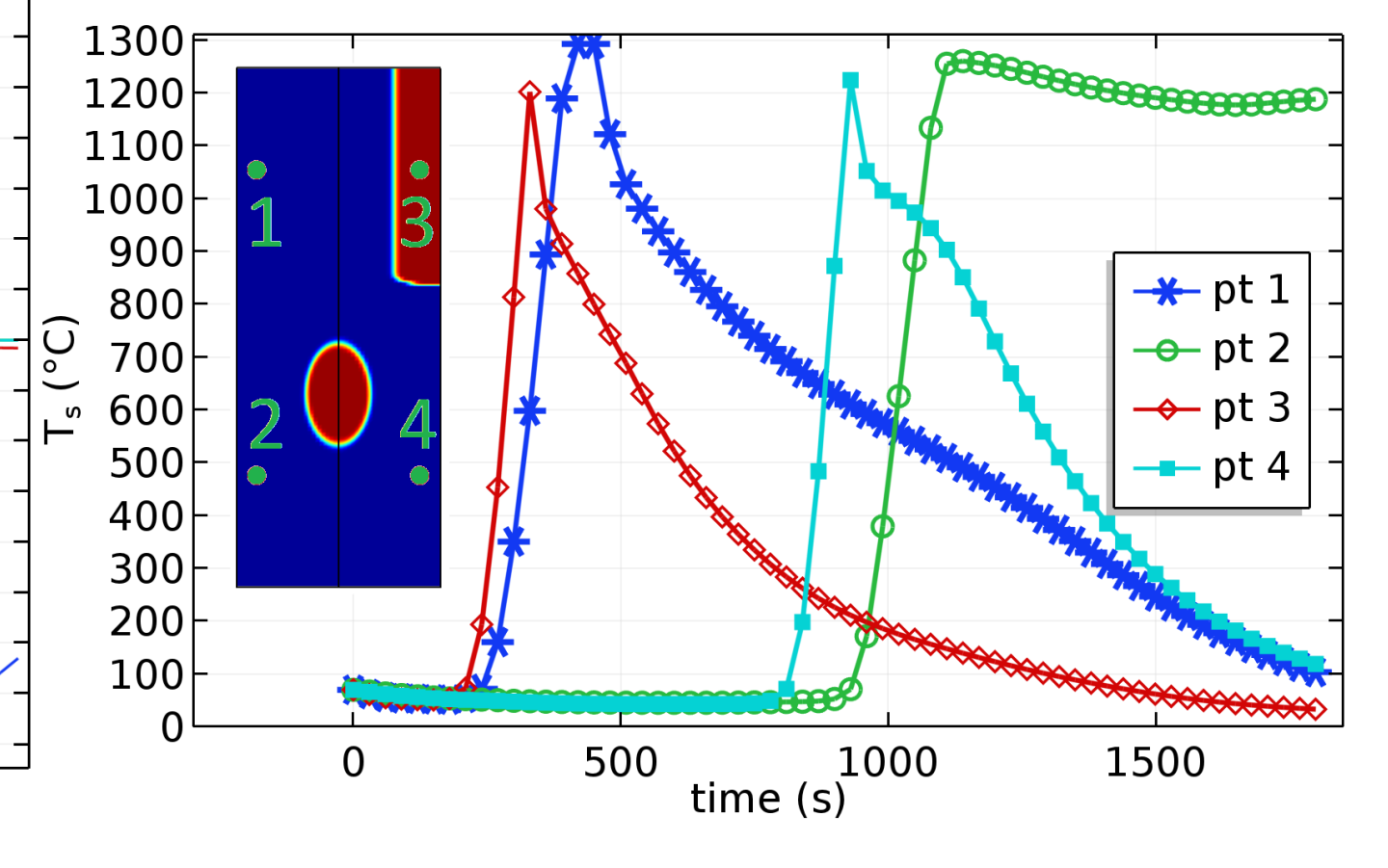


Figure 4. Time-temperature curves

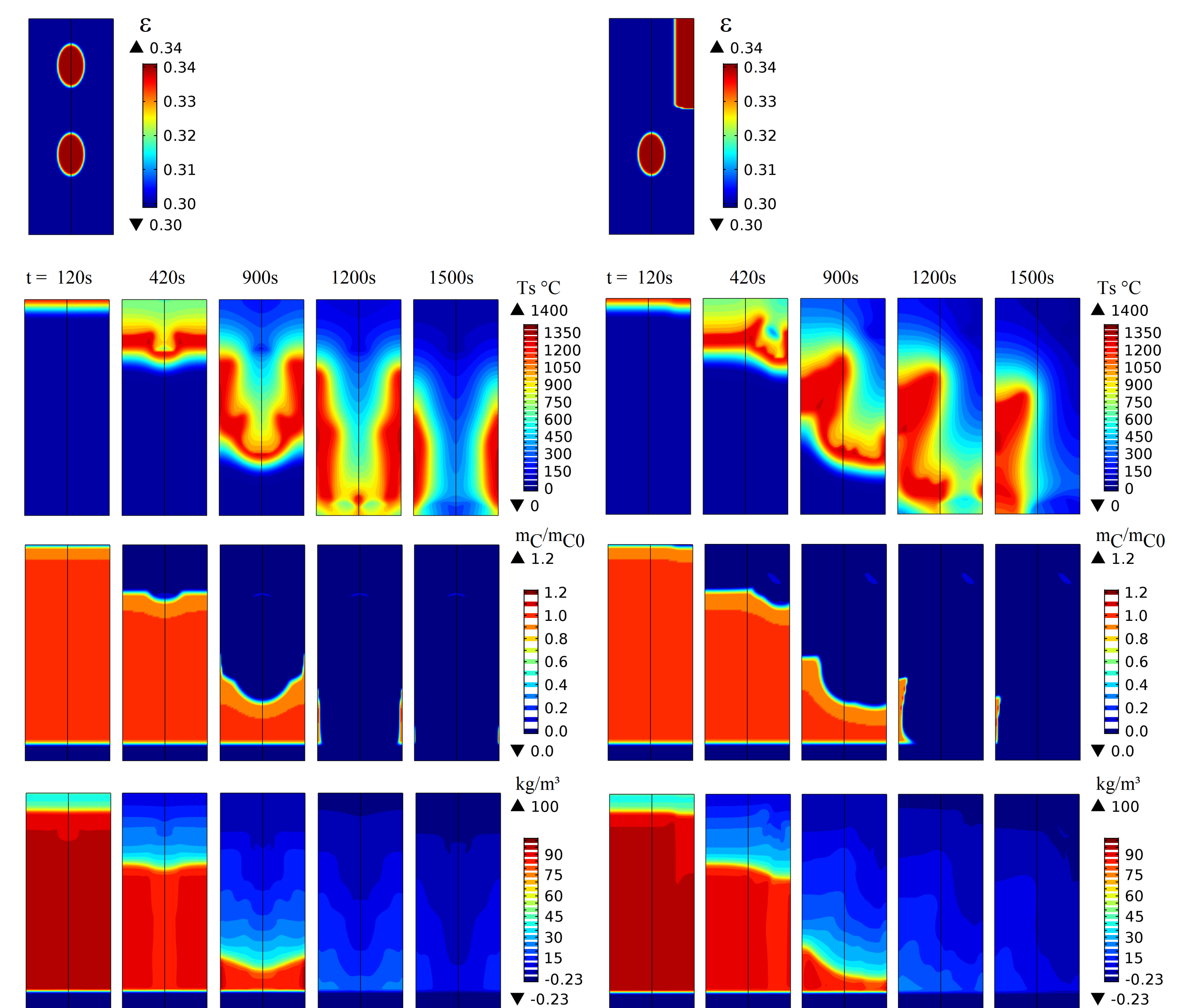


Figure 5. Comparison of the permeability bar configurations and sinter process progress

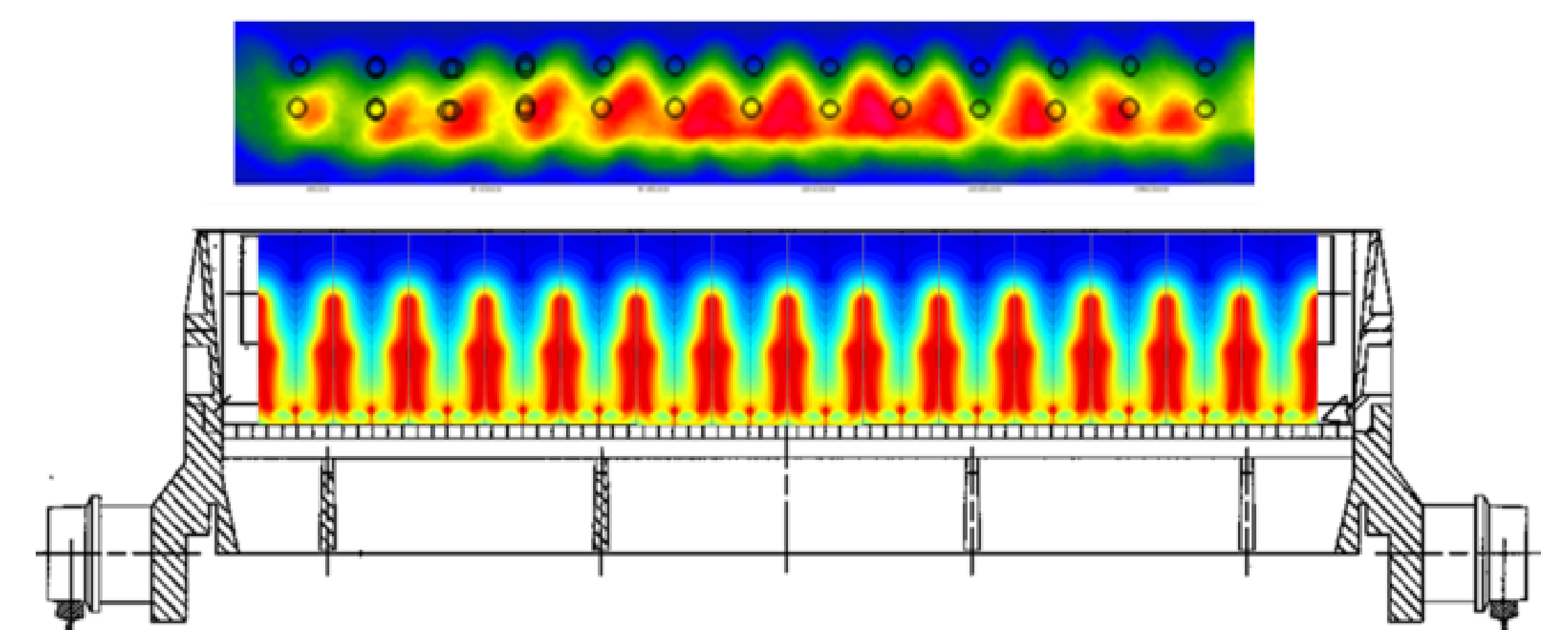


Figure 6. Comparison of the simulated and measured high temperature zone at discharge

Conclusions: Process speed can be raised by up to 40% with optimum permeability bar configuration. Optimum results were obtained either with two stacked rows of horizontal bars or with vertical bars & horizontal bars in-between. The bar design should be supported by the statistical analysis of the thermal profiles at discharge. The average sinter strength (quality) usually decreases slightly.

As future work, the model can be extended to include the influence of the diffusion and the dispersion phenomena in the convection equations. Moreover, a sub-model for the NOx emission can be implemented. Furthermore, the set of the chemical reactions and the involved species can be extended to increase model accuracy and capabilities. Implementation of a user friendly app-interface for the plant operators would be also worthy.

References:

1. T. Hauck, et. al., Optimisation of permeability bars to customise sinter plants on changing demands, 1-146, European Commission, Luxembourg (2017)
2. F. Cappel, Sintern von Eisenerzen, Verlag Stahleisen M.B.H., Düsseldorf (1973)